Medical Research Archives

ESMED
European Society of Medicine

OPEN ACCESS

Published: March 31, 2023

Citation: Hullender DA, Brown OR, et al., 2023. Non-Invasive Blood Pressure Total Waveform Monitoring Using Information Extracted by an Extended Kalman Filter Algorithm from Pulsations in an Oscillatory Cuff, Medical Research Archives, [online] 11(3). https://doi.org/10.18103/mra.v11i3.3677

DOI
https://doi.org/10.18103/mra.v11i3.3677

ISSN: 2375-1924

RESEARCH ARTICLE

Non-Invasive Blood Pressure Total Waveform Monitoring Using Information Extracted by an Extended Kalman Filter Algorithm from Pulsations in an Oscillatory Cuff

David A. Hullender, Professor of Mechanical Engineering at the University of Texas at Arlington, Box 19023, 76019, USA.

Olen R. Brown, Professor Emeritus, Dalton Cardiovascular Research Center, University of Missouri.

Atul Shrotriya, Chief Robotics Engineer, EZ BOTS

*Correspondence: hullender@uta.edu

Author contribution
Professor Hullender developed the models and programed the code for simulating the EKF algorithm.
Professor Brown researched the literature and made a major contribution to writing the paper.
Atul Shrotriya researched the literature for cardiovascular risk factors that may be identified in a blood pressure waveform. He also contributed to writing the paper.

ABSTRACT

This paper describes a novel approach designed for non-invasive, routine screening of patients for cardiovascular disorders without the complexities of using an electrocardiogram or invasive probes. Specifically, an oscillographic-view of the brachial artery blood pressure waveform, including the dicrotic notch, is extracted from information in the pressure pulsations from an ordinary blood pressure cuff. The novelty of this approach is that the total continuous shape of the waveform, not just two numbers for pressures, is generated. A computer algorithm processes the cuff pressure pulsations and provides a near real-time visual estimate of the continuous shape of the blood pressure waveform to be viewed on oscilloscopes commonly used in hospitals and medical clinics. A model-based Extended Kalman Filter (EKF) algorithm is used to process the information and identify the coefficients of a Fourier transform model for the waveform and the coefficients for an empirical model for artery stiffness. By viewing the total waveform, variations or disorders in the waveform during a series of pulse cycles can be observed and easily recognized. Simulations of two-case studies demonstrate successful convergence of the algorithm for a variety of waveform disorders including arrhythmia, variations in the shape of the dicrotic notch, changing systolic and diastolic pressure levels, and stiff arteries. Experimental verification of this proposed procedure will require invasive pressure measurements while simultaneously processing the algorithm for non-invasive waveform comparisons. Once the algorithm is verified experimentally, the end goal is to use the procedure on patients with known cardiovascular diseases in order to easily create a database of waveform disorders correlated with disorders of specific cardiovascular diseases.

INTRODUCTION

Early detection of cardiovascular diseases is a primary area of research worldwide. Coronary artery disease, arrhythmias including atrial fibrillation and flutter, valvular heart disease, and causes of high blood pressure are areas of primary concern. Improved, convenient assessment methods suitable for screening in a clinic are desirable. This paper pertains to a proposed new non-invasive procedure for generating an oscillographic-continuous-view of the brachial artery blood pressure waveform including the dicrotic notch. Our approach is novel; we use a model-based Extended Kalman Filter algorithm to estimate the coefficients in proven models for artery elasticity, adiabatic compression of air in confined chambers, and Fourier series equations for periodic functions. The accuracy of the method is determined by the degree of minimization of a covariance matrix which is reflected in the convergence of the modeling coefficients to 'known' values. In this paper, the 'known' values correspond to values for a hypothetical waveform with disorders simulated for a patient. A simulation of the algorithm is the procedure for testing the algorithm. For actual clinical applications none of the values will be known. Successful convergence is demonstrated for two hypothetical patient's waveforms.

An accurate view of repeated pulse cycles in a waveform reveals variations in the systolic and diastolic pressure levels, variations in the shape of the waveform and variations in the pulse rate. This proposed simple non-invasive procedure would contribute significantly to the results of extensive efforts to correlate specific cardiovascular diseases to disorders in the blood pressure waveform[1,2]. Also, this proposed procedure would enhance the accuracy of values for the systolic and diastolic pressures which is of paramount importance according to the American College of Cardiology and the American Heart Association[3]. Recently issued guidelines lowered the definition of high blood pressure; approximately three-quarters of men over 65 years of age meet the criterion and are diagnosed as hypertensive[4]. A view of a waveform on an oscilloscope would reveal atrial fibrillation; a review in 2019 reported that atrial fibrillation affects approximately 3% of the general population in the U.S. and is twice as common in hypertensive patients[5].

Although most algorithms are proprietary, extensive documentation has been published pertaining to the accuracy of different types of sensors and algorithms used to measure non-invasively a patient's systolic and diastolic pressure levels[6-17]. However, the accuracy of estimates of these pressure levels may be difficult to assess for patients with atrial fibrillation, atrial flutter, skipped heart beats, and/or arterial stiffness. For a series of pulse cycles with variations in the pressure levels and pulse rate, estimates of numerical values of fiducial points in a patient's waveform may not be reliable using available algorithms; consider the waveform examples shown in Figure's 1 and 2.

Figure 1 shows a typical blood pressure waveform including the dicrotic notch for a systolic to diastolic ratio of 120/80 and pulse rate of 75 beats per minute[2]. The waveform is observed to be periodic with a time period of 0.8 s for each pulse cycle. Sophisticated non-invasive oscillatory algorithms would most likely provide accurate values for the pulse rate, systolic, and diastolic pressure levels for a consistent waveform such as this.

However, consider the hypothetical irregular waveform shown in Figure 2. A series of five-pulse cycles of a patient's waveform with a skipped beat, with variations in the pulse rate, and with varying levels of systolic and diastolic pressures is shown. Note that the first pulse cycle has a period of 1.2 s (50 beats/min.) but the next 2-cycles have periods of 0.6 s (100 beats/min.) with elevated pressures. These pulse cycles are followed by a 0.6 s 'quiet' period with no heartbeat which is followed by two additional pulse cycles with periods of 1.2 s and varying pressure levels. A view of this series of pulse cycles on an oscilloscope would be most informative.

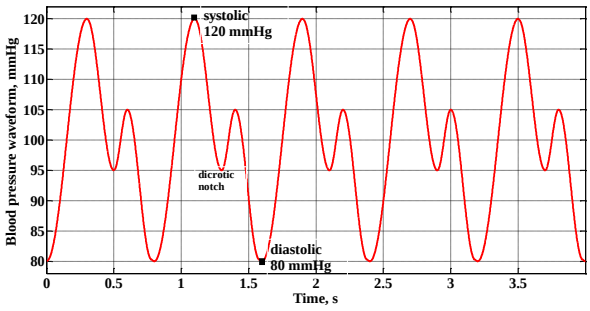

Figure 1. Five pulse cycles of an assumed healthy normal blood pressure brachial artery waveform with pulse cycle periods of 0.8 s (75 beats/minute) and pressure levels of 120/80

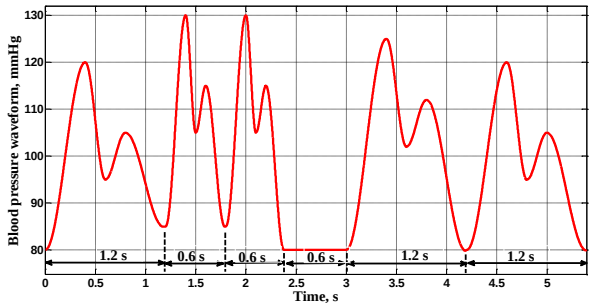

Figure 2. A hypothetical brachial artery waveform with atrial flutter, a skipped beat, and varying systolic and diastolic pressure levels

Using most commercially available non-invasive sensors, single numerical estimates of the systolic and diastolic pressure levels and of the patient's pulse rate would probably not be reliable for a waveform with irregularities such as in Figure 2. At best, average values would be provided. However, a graphical view on an oscilloscope of a waveform such as shown in Figure 2 would be very revealing in regard to assessing waveform disorders and cardiovascular issues. The objective of using the proposed EKF algorithm is to provide such a graphical view.

METHODS

The method used in this research is to simulate the identification of hypothetical waveforms with disorders using the EKF algorithm. To understand the procedure for obtaining an oscillographic view of a series of pulse cycles making up the blood pressure waveform, imagine a cuff being placed on the arm or wrist of a patient who has unknown blood pressure levels, an unknown heartbeat rhythm, and an unknown degree of artery stiffness. An external air pump is used to increase the air pressure in a conventional oscillatory cuff from zero to a max level and then decrease it back to zero with this cycle potentially repeated more than once. During this process, it is known that the changes in the artery volume associated with squeezing the artery with increased cuff pressure in conjunction with the changing blood pressure in the artery will induce small pressure oscillations in the cuff which can be measured; a mathematical model is utilized in the simulations to represent this phenomenon. Commercially-available blood pressure measuring devices use these pressure oscillations with proprietary algorithms to estimate the pulse rate and the systolic and diastolic pressure levels. In the proposed procedure in this paper, however, these pressure oscillations are the input to the EKF algorithm which creates the total continuous shape of the waveform for view on an oscilloscope revealing shape irregularities and disorders. An estimate of the degree of atrial stiffness is also an output of the algorithm; the level of arterial stiffness is based on a mathematical empirical model for arterial stiffness.

Previous research with the EKF method

Previously documented research using the EKF algorithm[18] pertains to an exploratory study to determine if enough information could be extracted from the cuff pressure pulsations to estimate a simple model for the blood pressure waveform. The model did not include the portion of a waveform associated with the dicrotic notch which adds additional model complexity affecting the number of terms in the equation for the Fourier series waveform model. Inclusion of the dicrotic notch does not change the EKF algorithm but it does change the preferred initial estimates of the unknown coefficients and potentially, the need for additional terms in the Fourier series. In the current paper, the initial estimates for the Fourier coefficients for the waveform do correspond to pulse cycles with a dicrotic notch.

Development and assessment of the model

The algorithm begins with initial estimates for the coefficients in the model for the shape of the blood pressure waveform during a pulse cycle and in the empirical model for arterial stiffness. As explained above, the input to the algorithm is the pressure pulsations in an oscillometric cuff commonly used to measure the systolic and diastolic pressure levels in the brachial artery. The algorithm extracts information from the cuff pressure pulsations and uses this information to adjust the estimates of the coefficients in the models so that they converge to coefficients corresponding to the patient's actual waveform and artery stiffness properties.

Equations for the cuff and the vessel stiffness models are developed below. These equations were previously formulated and published[18] and are included here for clarity and completeness. For purposes of simulating the process, the nominal cuff volume is assumed to exponentially change from an initial volume V_o at zero gage cuff pressure to a maximum volume V_{cm} at the maximum cuff pressure P_{cm}; the equation for these low frequency volume changes is shown in (1).

$$V_c(t) = V_o e^{-5\frac{P_c(t)}{P_{cm}}} + V_{cm}\left(1 - e^{-5\frac{P_c(t)}{P_{cm}}}\right) \qquad (1)$$

The equation for the derivative of the pressure oscillations in the cuff associated with artery volume changes is the difference in the adiabatic capacitance equations for the pressure in the cuff with and without consideration of the artery volume changes $\dot{V}_a(t)$. This is equation (2), i.e.

$$\dot{y}(t) = \frac{1.4P_{ca}}{V_c(t)}\dot{V}_a(t) \qquad (2)$$

where $P_{ca}(t)$ is the absolute pressure in the cuff.

The artery volume $V_a(t)$ is a function of the stiffness properties of the artery walls and the transmural pressure $P_t(t) = P(t) - P_c(t)$ on the artery walls where $P(t)$ is the blood pressure in the artery[13,19-22]. Thus, the equation for the derivative of the oscillations in the cuff pressure $y(t)$ due to changes in the artery volume becomes

$$\dot{y}(t) = \frac{1.4P_{ca}(t)}{V_c(t)}\dot{P}_t(t)V_{ao}f(P_t) \qquad (3)$$

where V_{ao} is the artery volume at zero transmural pressure; $f(P_t)$ represents the nonlinear discontinuous exponential compliance function for the walls of the artery[16-18], i.e.

$$f(P_t) = ae^{-bP_t(t)} \ \ for \ \ P_t(t) \geq 0 \qquad (4)$$
$$f(P_t) = ae^{aP_t(t)} \ \ for \ \ P_t(t) < 0 \qquad (5)$$

The coefficients a and b are empirical constants from actual data used to model artery wall compliance. Equations (3-5) represent the nonlinear model used in the formulation of the Jacobian matrix used to generate the continuous numerical solution to the EKF algorithm[23] using cuff pressure oscillations $y(t)$ for the input.

The degree of artery stiffness is indicated by the slope of the compliance function; the smaller the slope, the greater the change in transmural pressure required for a given change in artery volume, and thus, the stiffer the artery. The compliance function for different degrees of stiffness relative to normal are shown in Figure 3 for positive and negative transmural pressures[19-22].

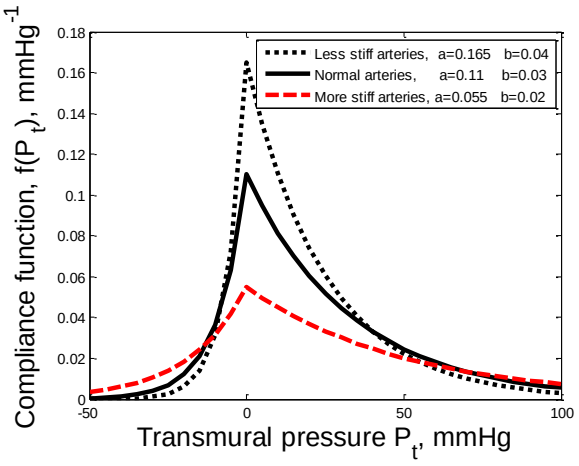

Figure 3. Compliance functions for varying degrees of artery stiffness relative to normal.

To estimate the blood pressure waveform $P(t)$ and its derivative $\dot{P}(t)$, a Fourier series with eleven unknown coefficients, A_i and B_i, and unknown frequency, ω, is used for the waveform model. The Fourier series is shown in (6).

$$P(t) = A_0 + A_1\,sin(\omega t) + A_2\,sin(2\omega t) + A_3\,sin(3\omega t) + A_4\,sin(4\omega t) + A_5\,sin(5\omega t) + B_1 cos(\omega t) + B_2\,cos(2\omega t) + B_3\,cos(3\omega t) + B_4 cos\,(4\omega t) + B_5\,cos(5\omega t) \qquad (6)$$

The compliance function $f(P_t)$ in (4) and (5) contains three unknown parameters a, V_{ao} and b to be estimated. The oscillations in the cuff pressure, $y(t)$, must also be estimated since the measurements of $y(t)$ may contain noise. Thus, there are eleven Fourier coefficients, the frequency ω, the artery parameters a, V_{ao} and b, and $y(t)$ being estimated in order to obtain estimates of the blood pressure waveform and stiffness properties of the artery. It is possible that the inclusion of the dicrotic notch may require additional terms in (6) for the Fourier series.

Equations (3-5) are nonlinear; thus, for purposes of simplifying the simulations, the continuous version of the EKF algorithm with the Jacobian matrix obtained from the partial derivatives of (3-5) is utilized. Actual hardware implementation, however, would utilize the discrete-time formulation of the algorithm since an A/D converter would be used to sample the cuff pressure oscillations and a microprocessor used to perform the computations. To determine the potential of the method, in this preliminary study no sensor or environmental noise was added to the measurements of $y(t)$.

The covariance matrix for estimating sixteen parameters and variables requires the numerical simulation of 136 simultaneous first-order differential equations; the covariance matrix defines the statistical uncertainties and interdependence of the constants and variables being estimated. Sixteen additional differential equations are required to compute the actual estimates and two additional differential equations are required for simulating $y(t)$ and $P_c(t)$. A variable step numerical integration algorithm was used for all simulations. As mentioned above, in each case, the cuff pressure starts at zero gage pressure and increases at an assumed rate of 10 mm Hg/s; after 16 seconds, the cuff pressure decreases at the rate of 10 mm Hg/s. These pressure rates were simply selected for the simulations but most certainly should be optimized for an actual hardware implementation. The cycle is repeated for cases requiring additional time for the estimates to converge to the true values.

For each simulation, initial coefficient estimates associated with the waveform to be identified must be assumed. In this study, these initial estimates correspond to a typical normal arterial blood pressure waveform with a systolic to diastolic ratio of 120/80 and a heartbeat frequency of 75 beats per minute. Initial estimates for stiffness properties correspond to empirical values from data for a normal artery defined in Figure 3.

The first step in the estimation process may require that an estimate of the patient's pulse rate be obtained. For relatively high pulse rates, a relatively accurate initial estimate of the pulse frequency may significantly reduce the time required and enhance the convergence of the estimates of all the coefficients using the EKF algorithm; this was not required for these case studies.

RESULTS

The actual shape and details of the hypothetical arterial blood pressure waveform reveals variations in rhythm, variations in the systolic and diastolic levels, disorders associated with the shape of the dicrotic notch, and variations in the volume of blood being pumped from the heart that may be associated with valvular issues[17]. In addition, changes in the shape of a patient's waveform between physical examinations may reveal the onset of cardiovascular issues and be valuable for early diagnosis and treatment[1].

Simulations testing the algorithm

Simulations for two patients' hypothetical waveforms have been generated to demonstrate the potential of using the EKF algorithm.

Case 1

Case 1 is a hypothetical waveform for a patient with relatively stiff arteries (Figure 3), a rapid pulse rate of 180 beats/minute, and systolic/diastolic pressures of 160/100. Figure 4 compares the patient's actual blood pressure waveform with a 'normal' waveform representing the initial estimate of the waveform at the beginning of the EKF simulation; note the significant differences in pressure levels and pulse rates. The results of the simulation are observed in Figure 5; the estimated coefficients in the models have sufficiently converged to a set that accurately estimates the pressure levels and pulse rate of the patient's actual waveform.

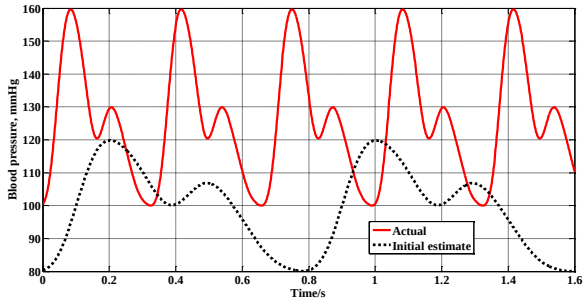

Figure 4. Patient's actual blood pressure waveform compared to the initial estimate

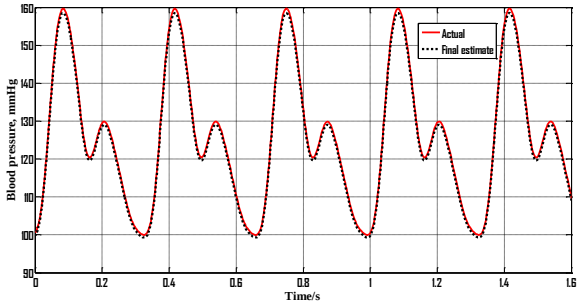

Figure 5. Patient's actual blood pressure waveform compared to the final estimate

The convergence of the modeling coefficients during the EKF simulation are shown in Figures 6-13 for Case 1. For the Fourier series, the coefficient estimates converge to sufficiently accurate values in approximately 20 seconds or less. As shown in Figure 12 for the artery stiffness model, the convergence of the coefficient estimates is somewhat erratic but apparently sufficiently accurate considering the comparison of the stiffness plots shown in Figure 13.

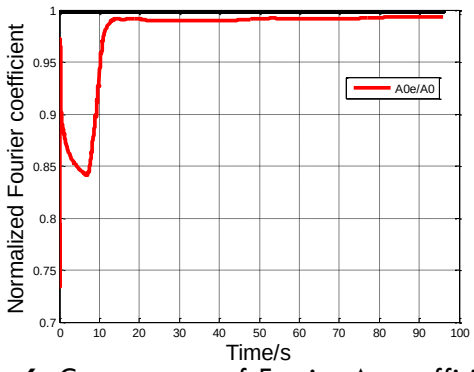

Figure 6. Convergence of Fourier A_0 coefficient

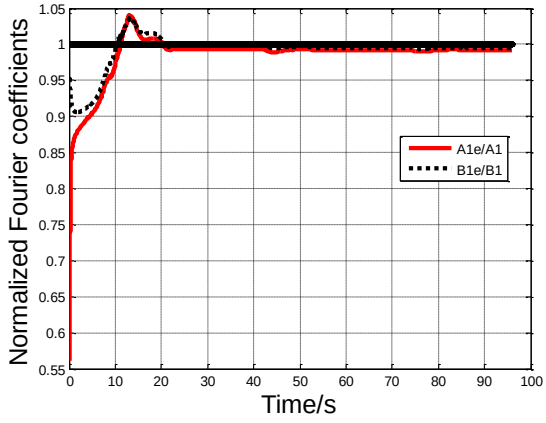

Figure 7. Convergence of A_1 and B_1 coefficients

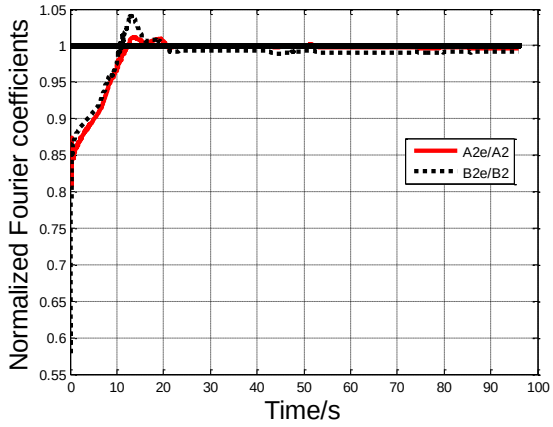

Figure 8. Convergence of A_2 and B_2 coefficients

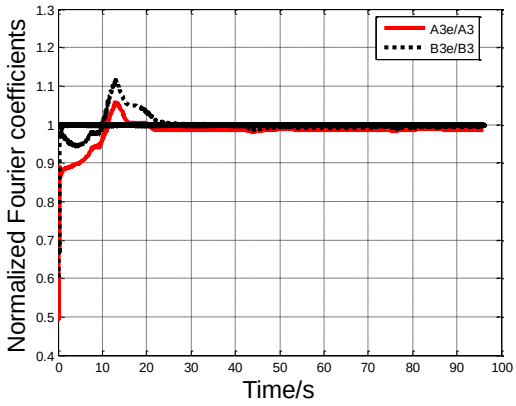

Figure 9. Convergence of A_3 and B_3 coefficients

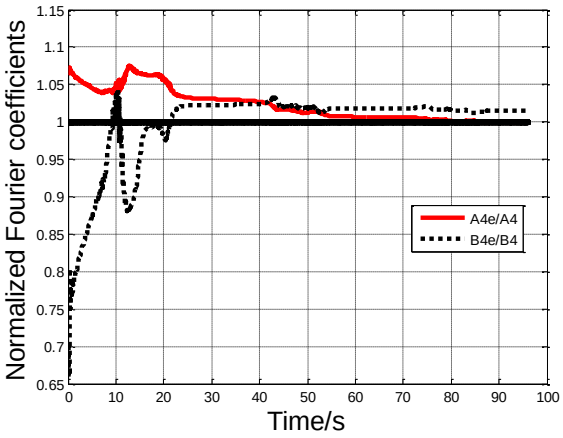

Figure 10. Convergence of A_4 and B_4 coefficients

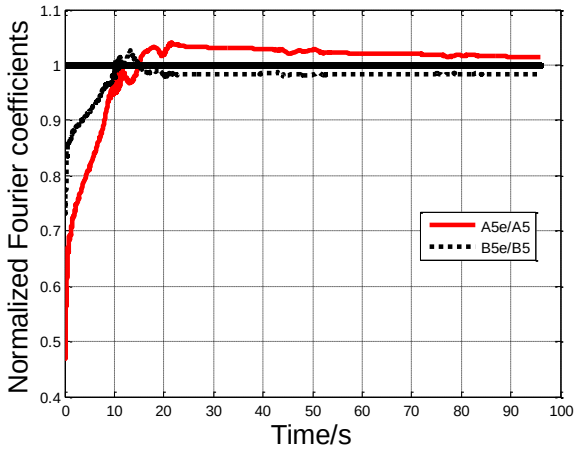

Figure 11. Convergence of A_5 and B_5 coefficients

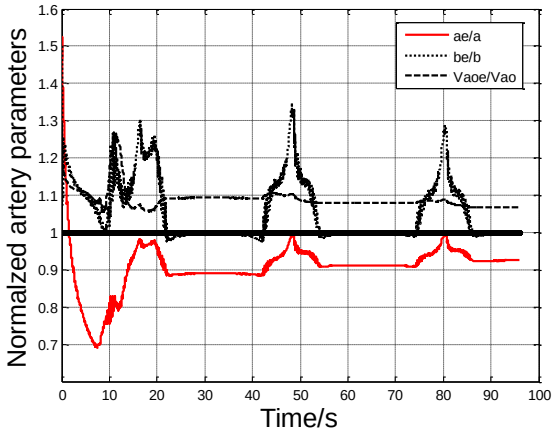

Figure 12. Convergence of stiffness model

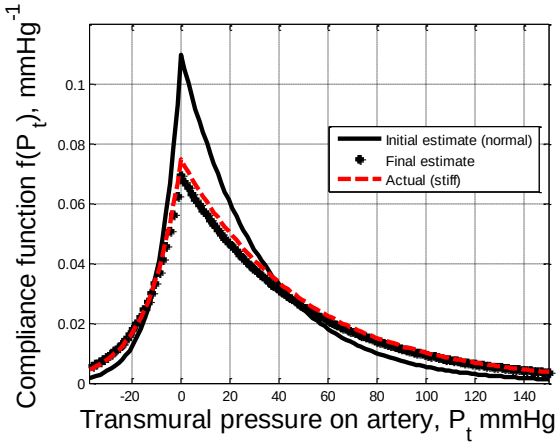

Figure 13. Stiffness convergence verification

Case 2

Case 2 is a hypothetical waveform for a patient with relatively stiff arteries (Figure 3), high blood pressure levels, a relatively high pulse rate, and a skipped heartbeat. As shown in Figure's 14 and 15, the results for Case 2 demonstrate that the EKF algorithm accurately converges from the initial estimate which is a normal waveform, 120/80 waveform with a pulse rate of 75 beats/minute, to the patient's actual waveform. The patient's waveform has pressures of 160/100, a pulse rate of 180 beats/minute, and a skipped heartbeat during the approximate time period of 0.3 to 0.65 seconds. Also, as shown in Figure 16, the EKF algorithm accurately converges from an initial estimate of a non-stiff artery model to the patient's actual stiff model. The convergence of all the coefficients for Case 2 are not shown.

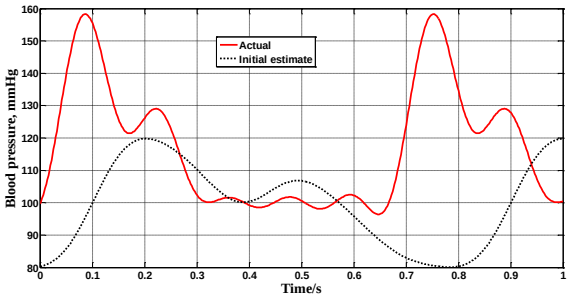

Figure 14. Patient's actual waveform compared to initial estimate

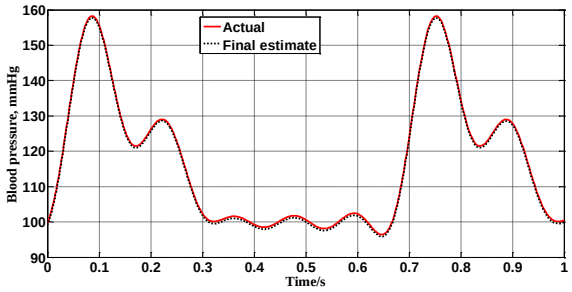

Figure 15. Patient's actual waveform compared to final estimate

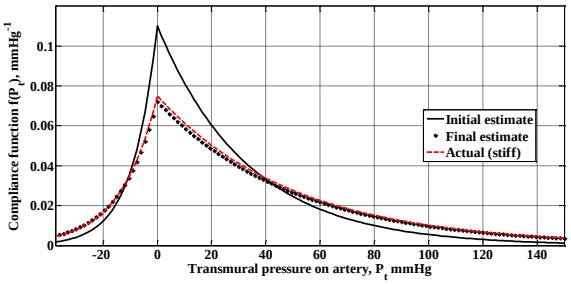

Figure 16. Convergence of the stiffness model estimate to the patient's actual model

DISCUSSION

Motivation

The motivation for this research has been to explore the potential of using the EKF algorithm in conjunction with a commercially-available oscillatory cuff, used for measuring blood pressure, to develop a low-cost, simple, non-invasive procedure for generating the continuous shape of the brachial arterial blood pressure waveform on an oscilloscope. Being able to see the continuous shape of the pulse cycles reveals arrhythmia and other irregularities associated with the waveform. Accurate observations of systolic and diastolic levels can be observed even if they are changing from pulse cycle to pulse cycle. The procedure provides a solution to the inaccuracy of conventional algorithms in non-invasive devices for estimating levels of blood pressure which are very dependent on the assumption of waveform regularity. For irregular waveforms such as shown in Figure 2, most currently available non-invasive devices would at best only be able to provide estimates of average values and the results probably would not be considered reliable. A graphical view of a continuous series of pulse cycles on an oscilloscope would be much more informative revealing disorders, variations, and other cardiovascular issues.

Once the algorithm is verified experimentally, the end goal is to use the procedure on patients

with known cardiovascular diseases in order to easily create a database of waveform disorders correlated with disorders of specific cardiovascular pathologies. For example, there are a number of time periods within a waveform which can be used to assess the cardiovascular health by comparison to themselves or other time spans[24,25]. One of the most important time periods is the pulse rate which represents the time duration of one complete blood pressure waveform pulse cycle. The pulse rate is associated and linked to atrial fibrillation and arrhythmia[26-29]. While hypertension indicates sustained high blood pressure levels, atrial fibrillation relates to irregular heart rhythm and is termed arrhythmia in a case of very rapid heart rhythm[30,31]. Although a visual representation of the waveform during a pulse cycle is not required to estimate the pulse rate, continuous monitoring of the waveform would potentially reveal the reasons for pulse rate estimate variations such as associated with skipped beats as well as valvular timing issues observed during the rise and descent of the pressure and the shape of the dicrotic notch.

The slope for pressure increases during systolic peak and the depth of the dicrotic notch, also referred to as incisura, are important factors of the blood pressure waveform [2,32]. These factors potentially can be used to predict the artery thickness, artery blockage, atrial valve function and other parameters important for assessment of cardiovascular health. When the aortic valve within the heart narrows abnormally, the condition is termed as aortic stenosis. According to many studies, this condition can be predicted by the small depth of the dicrotic notch or an indistinct incisura[33-35]. A comparison and continuous assessment of these shape and timing variables can potentially be used to diagnose arterial sclerosis, aortic stenosis, aortic regurgitation, hypertrophic obstructive cardiomyopathy, coronary artery disease, atrial fibrillation, and stroke.

As demonstrated in this paper, the EKF algorithm is model-based. This means that the EKF algorithm is attempting to identify values for coefficients in the mathematical model for the frequency components of the waveform and values for the coefficients in the empirical model for arterial stiffness. To test the algorithm, coefficients for a 'normal' waveform and coefficients for healthy arteries were assumed for initial estimates in the EKF algorithm. Plots demonstrating the change and convergence of the initial coefficient estimates to the coefficients of two different hypothetical arrhythmia waveforms were shown. The simulation results demonstrated the success of the algorithm for 2-case studies. The algorithm, however, does require that the model for the pressure cuff be representative of the particular hardware configuration of the cuff and that the patient's arteries comply with the empirical model for arterial stiffness. Also, noise levels on the cuff pressure measurements have been assumed to be minimal; the potential significance of measurement noise needs to be studied.

Proposed future research

The final verification of the procedure would be to correlate EKF generated waveforms with patients' actual waveforms. This will require simultaneous invasive recording of actual waveforms with waveforms generated with the EKF algorithm. In addition, assuming the procedure will be verified experimentally, a preliminary study[36] has been conducted considering previous research[37-41] to automatically assess the output of the EKF algorithm to potentially identify and rate risk factors associated with the waveform shape and cycle times mentioned in the paper; the results appear to be very promising and need to be continued with different pathologies.

CONCLUSION

This research is an extension of previous work to evaluate the potential of extracting information obtained from a non-invasive commercially available pressure cuff to create a visual estimate of the shape of the brachial artery blood pressure waveform including the dicrotic notch during a pulse cycle. Simulation results reveal the results to be very promising with a high level of robustness even when the complexities of the dicrotic notch have been included.

Conflicts of Interest: There are no conflicts of interest.

Submission Declaration: This is original research that has not been published previously nor is it being considered elsewhere.

Funding Declaration: This research did not receive any specific grant from funding agencies in the public, commercial, or not-for-profit sectors.

References

1. Anon. Syllabus for the Basic Sciences in Intensive Care Medicine, Section G7(iii), 2017 CICM Primary Syllabus. Published online 2017.
2. Nirmalan M, Dark PM. Broader applications of arterial pressure wave form analysis. *Continuing Education in Anaesthesia, Critical Care and Pain*. 2014;14(6):285-290. doi:10.1093/BJACEACCP/MKT078
3. Muntner P, Einhorn PT, Cushman WC, et al. The Present and Future Blood Pressure Assessment in Adults in Clinical Practice and Clinic-Based Research JACC Scientific Expert Panel. Published online 2019. doi:10.1016/j.jacc.2018.10.069
4. Anon. Blood pressure goals: How low should you go? Harvard Health Publishing, Harvard Medical School. Published 2019. https://www.health.harvard.edu/mens-health/blood-pressure-goals-how-low-should-you-go
5. Verberk WJ, de Leeuw PW. Accuracy of oscillometric blood pressure monitors for the detection of atrial fibrillation: A systematic review. *Expert Rev Med Devices*. 2012;9(6):635-640. doi:10.1586/erd.12.46
6. O'brien E, Waeber B, Parati G, Staessen J, Myers MG. *Clinical Review Blood Pressure Measuring Devices: Recommendations of the European Society of Hypertension*.
7. Egmond J van, Lenders JWM, Weernink E, Thien T. Accuracy and Reproducibility of 30 Devices for Self-Measurement of Arterial Blood Pressure. *Am J Hypertens*. 1993;6(10):873-879. doi:10.1093/ajh/6.10.873
8. Vischer A, Burkard T. *Principles of Blood Pressure Measurement – Current Techniques, Office vs Ambulatory Blood Pressure Measurement.*; 2016.
9. Forouzanfar M, Dajani HR, Groza VZ, Bolic M, Rajan S, Batkin I. Oscillometric blood pressure estimation: Past, present, and future. *IEEE Rev Biomed Eng*. 2015;8:44-63. doi:10.1109/RBME.2015.2434215
10. Balestrieri E, Daponte P, Vito L de, Picariello F, Rapuano S. Oscillometric blood pressure waveform analysis: challenges and developments. *IEEE*. Published online 2019.
11. Abiri A, Chou EF, Qian C, Rinehart J, Khine M. Intra-beat biomarker for accurate continuous non-invasive blood pressure monitoring. *Scientific Reports 2022 12:1*. 2022;12(1):1-13. doi:10.1038/s41598-022-19096-6
12. Singh O, Sunkaria RK. Detection of Onset, Systolic Peak and Dicrotic Notch in Arterial Blood Pressure Pulses. *Measurement and Control (United Kingdom)*. 2017;50(7-8):170-176. doi:10.1177/0020294017729958
13. Komine H, Asai Y, Yokoi T, Yoshizawa M. Non-invasive assessment of arterial stiffness using oscillometric blood pressure measurement. *Biomed Eng Online*. 2012;11. doi:10.1186/1475-925X-11-6
14. Antsiperov VE, Mansurov GK, Danilychev M v., Churikov D v. Non-Invasive Blood Pressure Monitoring with Positionable Three-chamber Pneumatic Sensor. *Proceedings of the 12th International Joint Conference on Biomedical Engineering Systems and Technologies (BIOSTEC 2019), pages 462-465*. Published online 2019:462-465.
15. Secomb TW, Castiglioni P, Don F, et al. Formulas to Explain Popular Oscillometric Blood Pressure Estimation Algorithms. *Frontiers in Physiology | www.frontiersin.org*. 2019;10:1415. doi:10.3389/fphys.2019.01415
16. Avbelj V. Morphological changes of pressure pulses in oscillometric non-invasive blood pressure measurements. In: *2014 37th International Convention on Information and Communication Technology, Electronics and Microelectronics, MIPRO 2014 - Proceedings*. IEEE Computer Society; 2014:245-248. doi:10.1109/MIPRO.2014.6859569
17. Lowe A, Oh TH, Stewart R. Screening for Atrial Fibrillation during Automatic Blood Pressure Measurements. *IEEE J Transl Eng Health Med*. 2018;6. doi:10.1109/JTEHM.2018.2869609
18. Hullender DA, Brown OR. Simulations of blood pressure and identification of atrial fibrillation and arterial stiffness using an extended Kalman filter with oscillometric pulsation measurements. *Comput Methods Programs Biomed*. 2021;198. doi:10.1016/j.cmpb.2020.105768
19. Segers P, Rietzschel ER, Chirinos JA. How to Measure Arterial Stiffness in Humans. *Arterioscler Thromb Vasc Biol*. 2020;40:1034-1043. doi:10.1161/ATVBAHA.119.313132/FORMAT/EPUB
20. Jeon A, Ro J, Kim J, Baik S, Jeon G. Simulation of the Blood Pressure Estimation Using the Artery Compliance Model and Pulsation Waveform Model. *Journal of Sensor Science*

and Technology. 2013;22(1):38-43. doi:10.5369/JSST.2013.22.1.38

21. Babbs CF. *Oscillometric Measurement of Systolic and Diastolic Blood Pressures Validated in a Physiologic Mathematical Model*. Vol 11.; 2012. doi:10.1186/1475-925X-11-56
22. Geddes LA, Baker LE. Principles of Applied Biomedical Instrumentation. Published 1975. Accessed December 10, 2019. https://www.bookdepository.com/Principles-Applied-Biomedical-Instrumentation-L-Geddes/9780471608998
23. Lewis F. *"Optimal Estimation with an Introduction to Stochastic Control Theory."* John Wiley & Sons, New York; 1986. Accessed December 10, 2019. https://www.scirp.org/reference/ReferencesPapers.aspx?ReferenceID=132449
24. Dawber TR, Thomas HE, Mcnamara PM. Characteristics of the dicrotic notch of the arterial pulse wave in coronary heart disease. *Angiology*. 1973;24(4). doi:10.1177/000331977302400407
25. Wood P. Aortic stenosis. *Am J Cardiol*. 1958;1(5). doi:10.1016/0002-9149(58)90138-3
26. Jain SK, Bhaumik B. An Energy Efficient ECG Signal Processor Detecting Cardiovascular Diseases on Smartphone. *IEEE Trans Biomed Circuits Syst*. 2017;11(2). doi:10.1109/TBCAS.2016.2592382
27. Garcia D, Pibarot P, Kadem L, Durand LG. Respective impacts of aortic stenosis and systemic hypertension on left ventricular hypertrophy. *J Biomech*. 2007;40(5). doi:10.1016/j.jbiomech.2006.03.020
28. Luz EJ da S, Schwartz WR, Cámara-Chávez G, Menotti D. ECG-based heartbeat classification for arrhythmia detection: A survey. *Comput Methods Programs Biomed*. 2016;127. doi:10.1016/j.cmpb.2015.12.008
29. Thakor N v., Zhu YS. Applications of Adaptive Filtering to ECG Analysis: Noise Cancellation and Arrhythmia Detection. *IEEE Trans Biomed Eng*. 1991;38(8). doi:10.1109/10.83591
30. Chazova IE, Golitsyn SP, Zhernakova J v., et al. Management of patients with arterial hypertension and atrial fibrillation. *Systemic Hypertension*. 2021;18(3). doi:10.26442/2075082x.2021.3.201077
31. Nattel S. New ideas about atrial fibrillation 50 years on. *Nature*. 2002;415(6868). doi:10.1038/415219a
32. Mills NL, Miller JJ, Anand A, et al. Increased arterial stiffness in patients with chronic obstructive pulmonary disease: a mechanism for increased cardiovascular risk. Published online 2007. doi:10.1136/thx.2007.083493
33. Sabbah HN, Stein PD. Valve origin of the aortic incisura. *Am J Cardiol*. 1978;41(1). doi:10.1016/0002-9149(78)90128-5
34. Mark JB. Atlas of Cardiovascular Monitoring. Churchill Livingstone Inc., New York, NY. 1998. ISBN:0-443-08891-8.
35. Judge TP, Kennedy JW. Estimation of aortic regurgitation by diastolic pulse wave analysis. *Circulation*. 1970;41(4). doi:10.1161/01.CIR.41.4.659
36. Shrotriya A. Analysis of Blood Pressure Waveform for Detection and Diagnosis of Cardiovascular Disorders. Dec. 12, 2021. Libraries Research Commons, University of Texas Arlington, dc.creator.orcid 0000-0002-5423-043X.
37. Jablonski I, Glomb G, Morello R. A Laboratory Set-up for Experimentation with the Cuffless Blood Pressure Measurement. In: *IEEE Medical Measurements and Applications, MeMeA 2020 - Conference Proceedings*. 2020. doi:10.1109/MeMeA49120.2020.913712
38. Sánchez R, Pessana F, Lev G, et al. Central Blood Pressure Waves Assessment: A Validation Study of Non-invasive Aortic Pressure Measurement in Human Beings. *High Blood Pressure and Cardiovascular Prevention*. 2020;27(2). doi:10.1007/s40292-020-00371-4
39. Moxham I. Physics of Invasive Blood Pressure Monitoring. *Southern African Journal of Anaesthesia and Analgesia*. 2003;9(1):33-38. doi:10.1080/22201173.2003.10872990
40. Mittnacht AJC, Kurki TSO. Arterial pressure monitoring. *Monitoring in Anesthesia and Perioperative Care*. Published online January 1, 2011:45-56. doi:10.1017/CBO9780511974083.008
41. Sackl-Pietsch E. Continuous non-invasive arterial pressure shows high accuracy in comparison to invasive intra-arterial blood pressure measurement. Medicine 2008. Corpus ID: 30046018. https://www.semanticscholar.org/paper/Continuous-non-invasive-arterial-pressure-shows-in/dde63d9510a7f9b0ff258e9b0cafdf150dfb8dc7